Essential Readings in Light Metals: Aluminum Reduction Technology.
Edited by Geoff Bearne, Marc Dupuis and Gary Tarcy.

Light Metals — From *Light Metals 1992*, Euel R. Cutshall, Editor

THE INTERACTION BETWEEN CURRENT EFFICIENCY AND ENERGY BALANCE IN ALUMINIUM REDUCTION CELLS

Fiona J. Stevens[1], Weidong Zhang[2], Mark P. Taylor[1], John J.J. Chen

1. Comalco Research Centre, Thomastown, Victoria 3074, Australia
2. Chemical and Materials Engineering Department, University of Auckland, New Zealand

ABSTRACT

In aluminium reduction cells the current efficiency interacts with the energy balance through both the thermodynamics and the hydrodynamics of the reduction process.

The overall enthalpy for the reduction reaction is endothermic and increases with current efficiency due to lower heat evolution from the re-oxidation reaction. Changes in current efficiency due to changed mass transfer conditions will lead to an energy deficit or surplus. This will occur predominantly in the electrolyte channels where the largest proportion of mass transfer-driven current efficiency loss occurs. Other sources of current efficiency loss such as electronic loss of faradaic current will further reduce the endothermic contribution of the reaction enthalpy and may cause localised energy surpluses.

The energy balance directly affects the electrolyte temperature and composition. It also affects the volume of the liquid electrolyte and the shape and thickness of side freeze and crust, which determine the shape of the operating cavity. Bath composition and temperature determine the physical properties of the electrolyte which, along with the geometry of the flow cavity, influence the turbulence of the bubble-driven circulation and the disturbance to the electrolyte-metal interface. Both factors influence the mass transfer and hence, metal re-oxidation rate.

1. INTRODUCTION

Previous measurement-based research on current efficiency has emphasised the phenomenological effect of process variables such as temperature, $A\ell_2O_3$, excess $A\ell F_3$ and ACD on the current efficiency but has not shown why these variables affect current efficiency, or what additional, interactive effects are present during the current efficiency measurements.

In more theoretical studies concerned with the mechanism of current efficiency loss, emphasis has been placed here on the hydrodynamics of the metal interface in determining the source of current efficiency loss. Various models for CE loss have been proposed previously[1,2], each assuming that a particular step in the metal loss process is rate-determining.

One missing element in these studies is the effect of changing current efficiency on other aspects of cell operation. In aluminium reduction cells there is a two-way interaction between current efficiency and the energy balance of the cell. The energy balance directly affects the operating bath chemistry and temperature and also the shape of the liquid cavity, in terms of ledge shape, side-channel width, ACD, sludge and ridge on the cathode and also bath height. These parameters then impact on the current efficiency by altering the mass transfer characteristics between the bath and metal phases. However the altered rate of metal re-oxidation also influences the energy balance since the overall enthalpy for the reduction reaction is endothermic and increases with current efficiency due to lower heat evolution from aluminium oxidation. In this way increases in cell current efficiency will result in an energy deficit and visa versa. It is important to note that increases or decreases in current efficiency can be reinforced and possibly accelerated by these subsequent changes in energy balance.

Although current density and metal production are concentrated in the ACD electrolyte regions, analogue modelling experiments[3] show that metal reoxidation is not. The degree of turbulence is much higher in the electrolyte channels and a large proportion of the mass-transfer driven metal loss occurs here - distant from the location of the forward electrolysis reaction. In this way the energy surplus or deficit due to current efficiency change may be localised. Current density variations around the cell will accentuate these local mass transfer differences by magnifying or reducing local electrolyte turbulence further.

Other sources of current efficiency loss, such as electronic loss of faradaic current, undoubtably occur and are sources of net ohmic heat production which further reduce the enthalpy requirement for the reduction reaction. These heating effects also tend to be localised under particular anodes in the cell.

2. MASS TRANSFER CONTROL OF CURRENT EFFICIENCY

In aluminium electrolysis the reoxidation of dissolved metal by anode gases is now widely accepted as being the major reason for current efficiency losses. The metal reoxidation or "back reaction" is generally believed to be controlled by mass transfer of the dissolved metal. The mass transfer process is a combined one which involves both gas/bath and metal/bath interfaces. Experimental results on a physical model[3] have shown that the mass transfer resistance at the gas/bath interface accounts for around 15% of the overall resistance to metal transport,

indicating that the mass transfer mechanism is dominated by the metal/bath interface.

A number of well-known models describing turbulent mass transfer at the interface between two fluids are available. The earliest film theory assumed a stagnant film adjacent to the interface on the solvent side (mass transfer resistance on this side of the interface only), in which stationary diffusion occurs and the mass transfer coefficient is proportional to the diffusion coefficient to the first power, $k \alpha D^{1.0}$. The penetration theory of Higbie[4] assumed unsteady diffusion into a liquid element residing at the interface for a short exposure time and Danckwerts[5] built on the approach, using a statistical distribution of the age's t, of the liquid element in the surface renewal theory. These penetration theories predict that $k \alpha (D/t)^{0.5}$. A combination of the film and penetration model by Toor and Marchello[6] gave $k \alpha D^{0.5\text{-}1.0}$, and was found to be better than the previous models when compared with their experimental data. Eddy diffusivity models have been adopted by most investigators in theoretical treatments. The eddy diffusivity model has the form, $D_t = ay^n$, where y is the distance measured normal to the interface, and a, n are experimentally determined parameters characterising the turbulence in the system of interest. Levich[7], and later Davies[8] assumed that the eddy scale of motion and the velocity fluctuations vary linearly with the distance from the interface so that $D_t \alpha y^2$. Through a force balance between the dynamic pressure fluctuation causing deformation of the interface (due to the eddy thrust) and the surface tension force opposing the deformation, the parameter, a, was deduced:

$$a \alpha (\rho D/\sigma_{equiv})(v^1)^3$$

in which v^1 is the turbulently fluctuating velocity in the bulk of the solvent phase, and σ_{equiv} = surface tension and gravitational pressure. The film mass transfer coefficient, k_L, was then derived by solving the steady-state mass transfer equation. Other models assuming surface tension, viscosity, or surface tension/viscosity damping mechanisms have also been proposed by subsequent investigators.

The relationships above for the mass transfer coefficient at a fluid/fluid interface all involve the hydrodynamic characteristics of the interfacial system. In particular the Levich-Davies relationship:

$$k_L \alpha \left(\frac{\rho D}{\sigma_{equiv}}\right)^{0.5} (v^1)^{1.5}$$

indicates that the turbulently fluctuating velocity component, v^1, will dominate the variation in k_L - a 20% change in v^1 causes a 31% change in mass transfer coefficient, k_L, compared to a 9% change in k_L for the same relative movement in diffusion coefficient, D.

Since the actual transport rate of aluminium across the interface, r_{Al}, is:

$$r_{Al} = k_L A_{Al} (C^*_{Al} - C_\infty) \qquad - (1)$$

it is clear that the solubility of the aluminium in the electrolyte, C^*_{Al}, is also an important parameter in the prediction of the absolute current efficiency. However the emphasis which has previously been placed on 'chemical control' via metal solubility and diffusion rate in the electrolyte is highly questionable, simply on the basis of the power dependence of v^1. This is particularly the case in quantifying the variation in current efficiency which should occur due to changes in operating parameters, since it is found experimentally that hydrodynamic conditions are a strong function of the cell operating parameters.

The studies using room temperature, analogue fluids have demonstrated that the release of large slugs of electrolytically produced gas from the periphery of the anodes causes high electrolyte turbulence in the channels and a transient fluctuation in the average fluid density near the point of release of the gas. The resulting large-scale eddies play an important role in determining the metal/electrolyte mass transfer coefficient as well as the gas/electrolyte
interfacial area due to entrained 'micro-bubbles' of gas. This latter effect needs to be accounted for in the calculation of overall mass transfer coefficient, K, for different electrolyte conditions.

The net affect of gas induced turbulence on the total mass transfer rate is at least a factor of two, within stable metal interfacial regimes. However under certain conditions of the cell cavity geometry, metal droplets may be sheared off the interface and entrained in the highly gasified cell channels. Under this unstable interfacial regime much higher overall mass transfer coefficients have been measured. These increases in mass transfer can occur without any changes in the fluid properties themselves, demonstrating that their origins are hydrodynamic rather than chemical in nature.

In real cells the delineation between pure hydrodynamic and chemical effects is more difficult to measure due to the simultaneous interaction of the energy balance with the cavity geometry and the fluid properties of the electrolyte (including diffusion coefficient and metal solubility). A change in energy balance which causes ledge to form and bath height to decrease will also cause aluminium fluoride concentration to increase and temperature to decrease in the electrolyte. Any one of these changes on its own will have an impact on the rate of back-reaction. The present work indicates that the combined effect of these changes on current efficiency often owes more to the altered hydrodynamic regime (v^1) than it does to the chemical parameters influencing transport of aluminium.

3. THE DYNAMIC ENERGY BALANCE

The conservation of energy (both internal and kinetic) for any system can be simply expressed as:

(Energy inflow - Energy Outflow) + Energy Production = Energy Accumulation - (2)

Normally a control volume or differential volume approach is used to apply equation (2) to a given system. However in multi-phase reactors such as reduction cells where the internal geometry, mass and volume of material are constantly changing, control volumes are quite difficult to define and a more flexible 'control system' framework is appropriate. Figures 1 and 2 show a control system discretization of the cell, and one of the

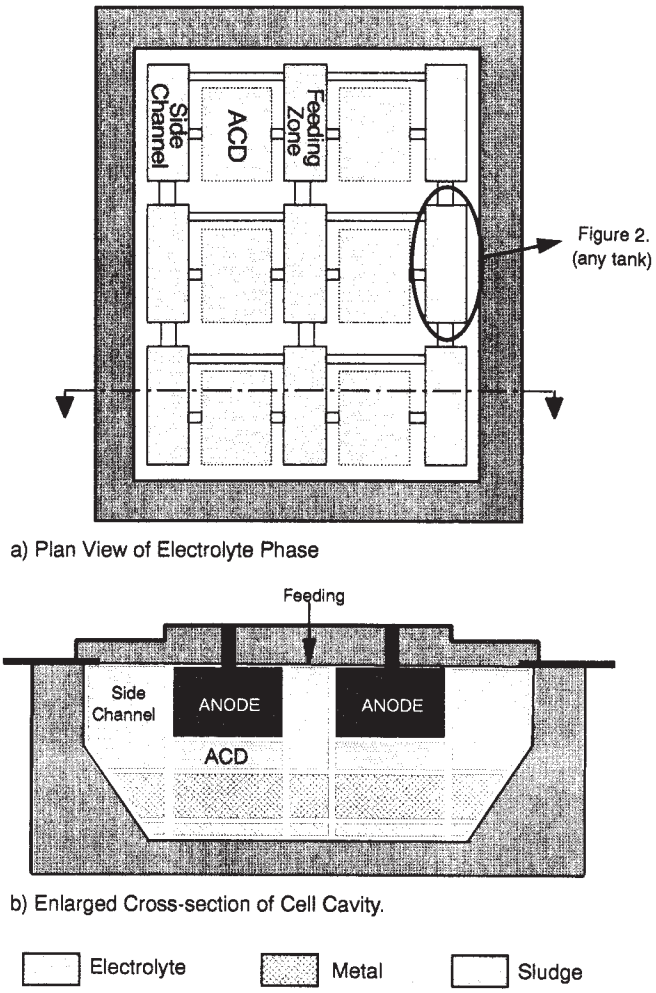

Figure 1. Continuous Stirred Tank Reactor Network for Reduction Cell.

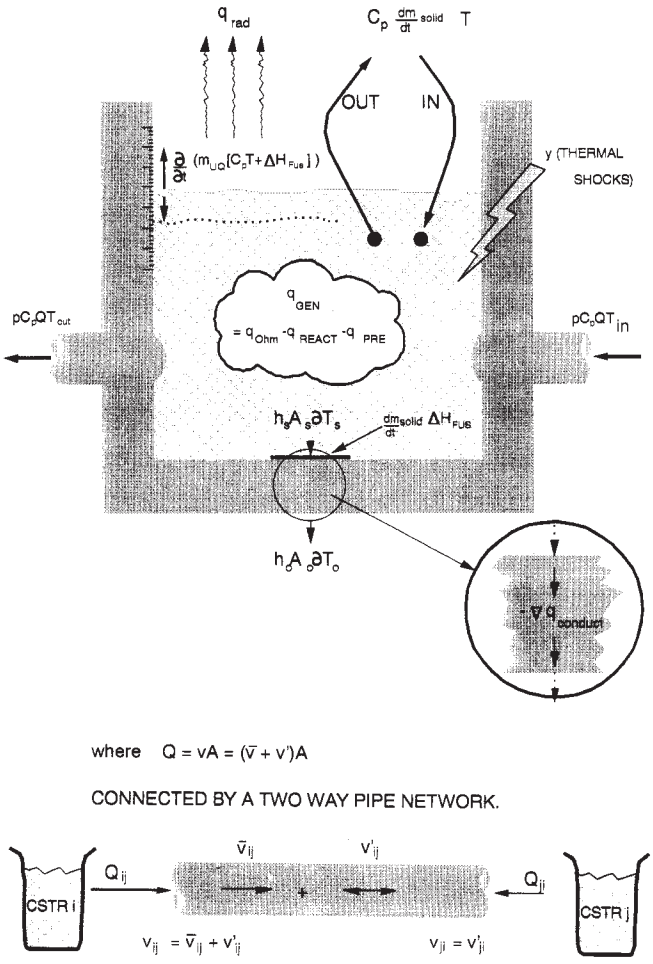

Figure 2. THE ENERGY BALANCE IN A CSTR Control System. (any tank in Figure 1.)

individual control systems respectively. The cell is viewed as a network of continuous stirred tank reactors (CSTR's) interlinked by pipes or channels through which fluid can be transported by both mean and turbulent components of the fluid flow. Each CSTR in the model is surrounded by solid materials representing the cell design as well as solidified electrolyte components such as ledge, crust and bottom ridge.

The energy equation (2) above is solved in both the liquid and solid cell materials along with the mass balance, phase equilibria and many process kinetic relationships which can impact on both sides of the energy equation. The localised nature of reduction cell operations such as feeding and anode setting, and the limited mixing which occurs in the electrolyte[3], both contribute to spatial non-uniformities as well as strong time-dependence in the basic cell operating parameters - including electrolyte temperature, composition, anodic current density and ledge/ridge profiles on the sidewalls and cathode. It is therefore to be expected that variations in the rate of metal back reaction will occur from place to place in the cell and also over time. Localised accumulation of sludge and cathode deposits in some areas (under feeders for example) exacerbate this variation in current efficiency and the resulting yellow flame near one or two anodes in a cell is a well known indicator of a localised problem.

Whether the source of current efficiency loss is related to loss of hydrodynamic stability, sludge accumulation or a spiked anode, the impact of the loss will be to increase the energy production term on the left-hand-side of EQ(2). In the case of sludge accumulation and/or spiked anodes, the magnification of the local heat production under an anode is very severe due to higher current density and ohmic heat generation. The resulting energy imbalance is worsened by large-scale metal recombination with anode gas, and by-passing or interruption of the endothermic forward electrolysis reaction for the production of aluminium (current shorting/electronic conduction).

Neglecting these 'catastrophic' losses in cell control and efficiency, which are becoming less common in state of the art smelters as operating practices and feeding systems improve, the impact of back-reaction alone on the energy balance can be quantified. For the total cell reaction:

$$1/2 \times A\ell_2O_3 \text{ (diss, T)} + 3/4 \text{ C (s,T)} = x \times A\ell_{(\ell,T)} + 3/4 (2x-1)CO_2 \text{ (g)} + 3/2 (1 - x) \text{ CO (g)} \quad \text{- (3)}$$

where: (1 - x) is the fractional loss in current efficiency due to mass transfer and re-oxidation of $A\ell$ by CO_2. CE = x.100

the enthalpy change is endothermic and is given by:

$$\Delta H_R = \Delta H_{FORWARD} + \Delta H_{BACK}\,(1 - x) \qquad - (4)$$

JANAF gives

$$\Delta H_{FORWARD} = 548{,}400 \text{ kJ/mole.A}\ell$$
$$\Delta H_{BACK} = -422{,}280 \text{ kJ/mole.A}\ell$$

at 977°C.

Multiplying this enthalpy change by the rate of electrolysis in the cell, the net power requirement to sustain electrolysis, q_R, is obtained:

$$q_R = \frac{I}{3F}\,(\Delta H_{FORWARD} + \Delta H_{BACK}\,(1 - x)) \qquad - (5)$$

The power requirement can be viewed as a negative 'energy production' term in the energy equation and is compensated for in a gross sense by the ohmic heat generation in the electrolyte. It is important to note, however, that ΔH_R is not related directly to the ohmic heat generation and that the reaction zones for the forward and back reactions are different, as discussed earlier. The potential exists therefore for a temporal and spatial imbalance in the energy production term.

Consider for example that the cell in Figure 1 operates at 90 kA with an electrolyte mass of 1500 kg and has 20 anodes. If its current efficiency drops uniformly around the cell from 94% to 89% due to increased aluminium transport into the electrolyte, q_R decreases from 162.6 kW to 156.1 kW, creating an energy surplus of 6.5 kW in EQ (2). However, because 5 m^2 of sidewall ledge area are available to the electrolyte through which the imbalance is distributed, dynamic energy balance predicts that ledge melting will begin to occur and will build up to a steady rate of 40 kg/hr with an accompanying increase in electrolyte superheat of only 1.5°C. These changes would be undetectable for some time within the total process variation occurring on an operating cell. Certainly, there is no significant thermal response predicted inside the cathode or sidewall insulation within a day of operation.

In contrast to this global loss of current efficiency, if the full 5% decrease in efficiency was due to breakdown of metal interface stability in the side-channel adjacent to two anodes, the same energy imbalance would be concentrated in a zone where only 50 kg of bath is present. In this case latent energy storage through ledge melting is initially insignificant, and almost all of the 6.5 kW imbalance accumulates as sensible heat in this small electrolyte zone. Depending on the velocity patterns and turbulence applied in the model between the different electrolyte regions, a temperature rise of 5-15°C is predicted in the low current efficiency zone. This temperature rise is not uniform along the length of the cell and subsequent ledge melting induces a complex thermal response through the cell due to the interaction between the changing bath composition, liquidus temperature and other cell processes (including current efficiency). The two-way, non-linear interaction between energy balance and current efficiency has been a major impediment to the understanding of both facets of reduction cell behaviour.

4. INDUSTRIAL CELL CURRENT EFFICIENCY

In a series of experiments conducted on a group of Comalco cells, the overall current efficiency over single tap cycles (32 hours) was measured using the radioisotope dilution technique[9]. During the measurement of current efficiency, four-hourly bath chemistry and temperature determinations were made. Average values for other process variables were also obtained.

A graph of measured current efficiency vs average bath temperature is shown in Figure 3 and a correlation is evident. A simple linear regression gives a 0.29% drop in current efficiency for a 1°C rise in bath temperature (r^2 = 0.42, significant at the 99% level). A graph of the measured current efficiency vs average % $A\ell F_3$ is shown in Figure 4 and in this case a strong correlation is evident. The data shows that an increase of 1.66% current efficiency occurs with a 1 wt % increase in excess $A\ell F_3$ (r^2 = 0.77, significant at 99% level).

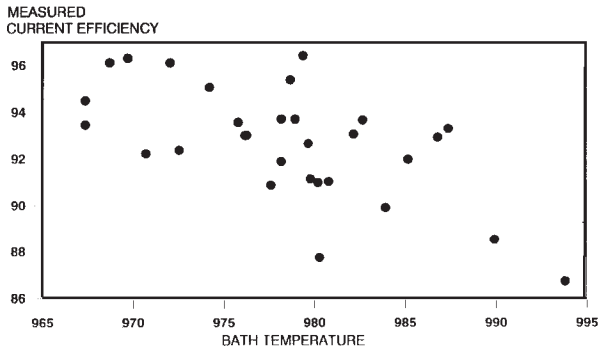

Figure 3
Influence of average bath temperature on current efficiency measured over 32 hour period

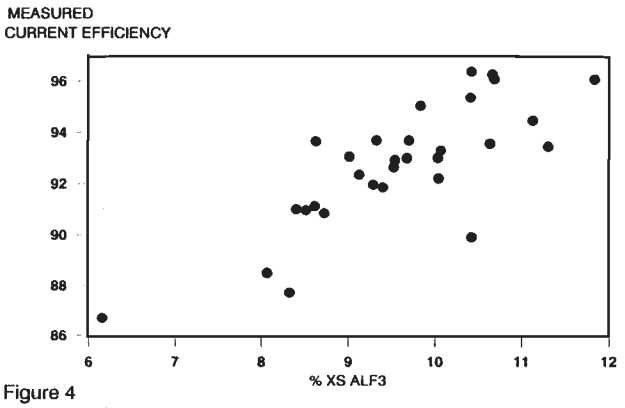

Figure 4
Influence of average % excess ALF_3 on current efficiency measured over 32 hour period

The effect of other bath components on current efficiency was considered and the results are summarised in Table 1. The data shows a correlation between current efficiency and $A\ell_2O_3$ concentration of only low significance. However this may be

Table 1: Correlation of Current Efficiency with wt% MgF_2, CaF_2 and $A\ell_2O_3$

	Sample Linear Regression		
Bath Component	% CE/wt%	r^2	Significance
MgF_2	+ 4.8	0.13	Significant at 95%
CaF_2	-	0.06	Not significant at 90%
$A\ell_2O_3$	-1.3	0.10	Significant at 90%

due to the average $A\ell_2O_3$ concentration not being adequately reflected in the four-hourly samples - the cycling frequency of $A\ell_2O_3$ concentration matches the alumina feeding cycle (~ 30 minutes).

A graph of average bath temperature against % excess $A\ell F_3$ is shown in Figure 5 and a definite correlation is evident (r^2 = 0.50, significant at 99% level). This interdependence of temperature and % excess $A\ell F_3$ occurs through the liquidus temperature. The dependence prevents determination of the primary parameter influencing current efficiency loss using statistical data correlation, as is the case with many sets of inter-related industrial data.

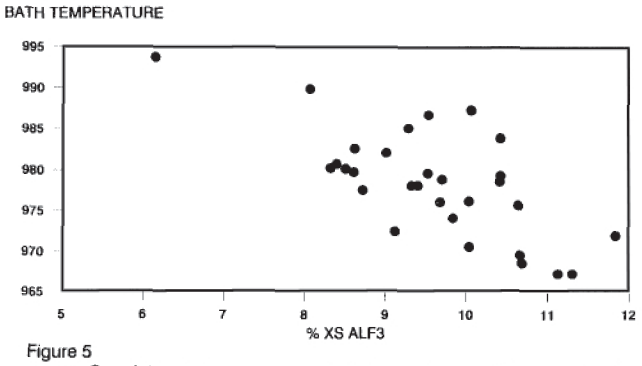

Figure 5
Correlation between average bath temperature and % excess ALF_3 during the periods of current efficiency measurement

A number of models for current efficiency loss have been documented in the literature. The predictive capability of these models can be assessed using the above set of industrial data. Lillebuen et al[1] assumed that convective transport through the bulk electrolyte was fast, and that concentration gradients only exist in the two stagnant films - at the bath-metal interface and the gas bubble-bath interface. They further assumed that the chemical reactions which form the reduced species in the melt occur very rapidly and that the metal re-oxidation reaction between the dissolved reactants occurs instantaneously. Simple film theory was used to describe the mass transfer relationships. The Lillibuen model gives the rate of aluminium loss by back-reaction as:

$$r_{A\ell} = 0.0204\ A_{A\ell}\ D_{A\ell}^{0.67}\ \ell^{-0.17}\ v^{0.83}\ \mu^{-0.5}\ \rho^{0.5}\ C^*_{A\ell}\ (1 - f) \qquad - (6)$$

Where:
- $r_{A\ell}$ = Rate of aluminium loss, mole/m³-S
- $D_{A\ell}$ = Difficulty of aluminium in the bath, m²/S
- ℓ = ACD, m
- v = interfacial velocity (metal-bath), m/s
- μ = viscosity of Bath, N/m².S
- ρ = density of bath, kg/m³
- $C^*_{A\ell}$ = solubility of bath, mol/m³
- f = aluminium concentration in the bath, as a fraction of the saturation solubility.

Similarly Evans et al[2] assumed that, near the bath-metal interface, momentum and dissolved aluminium transport are both damped by the interfacial tension, and that the mass transfer of dissolved species across the interface is rate controlling. They used the Levich equation to calculate the mass transfer of dissolved species through a surface tension induced boundary layer:

$$r_{A\ell} = \left(\frac{D_{A\ell}\rho}{\sigma}\right)^{0.5} k_t^{0.75}\ A_{A\ell}\ C^*_{A\ell} \qquad - (7)$$

where $D_{A\ell}$, ρ, $A_{A\ell}$ and $C^*_{A\ell}$ are as defined before, σ is the bath-metal surface tension and k_t is the turbulent kinetic energy due to the electromagnetic force field.

From both EQ (6) and (7), $r_{A\ell}$ can be used to calculate the current efficiency since:

$$CE = 100\left(1 - \frac{3F}{I}\ r_{A\ell}\right)\ \% \qquad - (8)$$

Comparisons of predicted and measured current efficiency are shown for each model in Figures 6 and 7. As both models assume that the total current efficiency loss is due to metal re-oxidation, the average predicted current efficiency has been set to the average measured current efficiency in the comparisons presented. In this way no estimations of v, k_t or f need to be made, and the ability of the models to explain changes in measured current efficiency can be assessed. Established physical property data[10,11] and recent data for total metal solubility[12] were used in all the model calculations.

The change in predicted current efficiency for each model is substantially lower than the measured variation. Lillebuen's model predicts 43% of the measured variation in current efficiency while Evans' model predicts 45%.

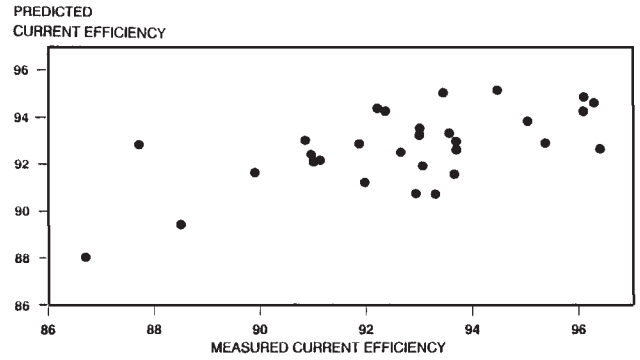

Figure 6
Comparision of the predicted current efficiency using Lillebuen's model with the measured current efficiency

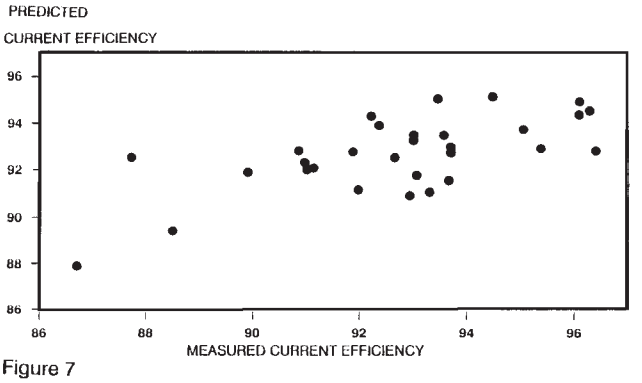

Figure 7
Comparision of the predicted current efficiency using Evans' model with the measured current efficiency

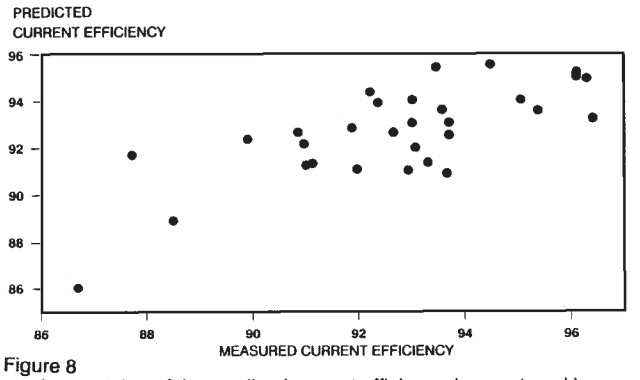

Figure 8
Comparision of the prediced current efficiency (present work) with the measured current efficiency

Both models concentrate on the (diffusive) mass transfer of aluminium across the interface. Lillebuen's model does not include changes in the convective transport in the bulk electrolyte or in the hydrodynamic characteristics at the interface and, similarly, the model of Evans does not account for the effect of gas-induced turbulence in the bath. The comparisons in Figures 6 and 7 highlight the inadequacies of these assumptions. Physical modelling work[13,14] has demonstrated the importance of gas-induced circulation in determining the level (and transient impact) of electrolyte turbulence. Based on this modelling, and dynamic similarity principles, a computational model for current efficiency loss is being developed, including the effect of gas induced turbulence. At the present state of development, 62% of the measured variation in current efficiency reported here is predicted by the model mass transfer relationships (Figure 8). Although the model was developed within a certain gas/electrolyte/metal interfacial regime, more recent physical modelling work has shown that other hydrodynamic regimes can arise through poor operation or widely fluctuating energy balance conditions. As indicated in Section 2, these regimes produce much higher and less predictable aluminium transfer rates, which very rapidly degrade current efficiency. These regimes may account for some of the unpredicted variation in current efficiency, particularly at the lower end of the current efficiency range.

5. IMPACT OF PROCESS VARIATION ON CURRENT EFFICIENCY

From the results of the industrial current efficiency measurements, it is evident that the combined impact of the cell energy balance, via average bath composition and temperature, on current efficiency is significant. It can also be shown, however, that the variation in energy balance is a determining factor in long term, average current efficiency. As an example we consider the variation in % excess $A\ell F_3$ concentration due to bath volume fluctuations.

Say X (t) = % excess $A\ell F_3$ at time t

We know CE = f (X), due to the aluminium mass transfer mechanism.

Now the average value of current efficiency over time interval t_1 is:

$$\overline{CE} = \frac{1}{t_1}\int_o^{t_1} f\,(X(t))\;dt \qquad \text{- (9)}$$

Using a Taylor expansion of f (X) about the average X in time t_1, $\bar{X}$

$$\overline{CE} \simeq \frac{1}{t_1}\int_o^{t_1}\left(f\,(\bar{X}) + (X(t) - \bar{X})\,f^1\,(\bar{X}) + \frac{(X(t)-\bar{X})^2}{2!}\,f^{11}\,(\bar{X})\right) \qquad \text{- (10)}$$

where f^1 and f^{11} are the first and second derivatives, respectively, of the function f.

$$\Rightarrow \qquad \overline{CE} \simeq f(\bar{X}) + f^1(\bar{X})\,\frac{1}{t_1}\int_o^{t_1}(X - \bar{X})\;dt \;+$$

$$f^{11}\,\frac{(\bar{X})}{2!}\,\frac{1}{t_1}\int_o^{t_1}(X - \bar{X})^2\;dt \qquad \text{- (11)}$$

Now $\int_o^{t_1}(X - \bar{X})\;dt = 0$

therefore

$$\overline{CE} = f(\bar{X}) + \frac{f^{11}(\bar{X})}{2}\,\frac{1}{t_1}\int_o^{t_1}(X - \bar{X})^2\;dt \qquad \text{- (12)}$$

Defining the terms in EQ (12):

$f(\bar{X})$ is the current efficiency at $\bar{X}$,

$\frac{1}{t_1}\int_o^{t_1}(X - \bar{X})^2\,dt$ is related to the variance in X, and is always positive.

The second derivative $f^{11}(X)$ therefore determines whether current efficiency is gained (+ve) or lost (-ve) due to the variation in parameter X. Clearly, for % excess $A\ell F_3$, f^{11} is negative due to the fact that CE rises with AℓF3 but cannot exceed 100%. (The rate of increase of CE with $A\ell F_3$ is therefore decreasing as the electrolyte becomes higher in $A\ell F_3$). The same argument applies equally well to the current efficiency increase as electrolyte temperature is reduced, and to other symptoms of energy balance fluctuation as well.

The above analysis shows that the degree of variation in the energy balance will impact on the average current efficiency through the non-linear nature of this relationship - the average current efficiency will decrease as the degree of variation increases even if the same average conditions are maintained. Serious variations in energy balance can, of course, cause gross changes in the internal cavity dimensions through ledge, ridge, bath or metal height variations. Even larger, more abrupt reductions in current efficiency are predicted under these conditions.

REFERENCES

1. B. Lillebuen et al, Electrochimica Acta., 25, 131 (1980).
2. J.W. Evans et al, Met. Trans., 12B, 353 (1981).
3. B.J. Welch, J.J.J. Chen, W.D. Zhang, J.M. Purdie, M.P. Taylor, Materials Science Forum Vol. 73-75, pp 779-787 (1991).
4. R. Higbie, Trans. AIChE, 32, 365 (1935).
5. P.V. Danckwerts, Ind. Eng. Chem., 43, 1460 (1951).
6. H.L. Toor, and J.M. Marchello, AIChE J., 4, 97 (1958).
7. V.G. Levich, Physicochemical Hydrodynamics, Prentice-Hall, Englewood Cliffs, New Jersey, 1962.
8. J.T. Davies, Turbulence Phenomena, Academic Press, N.Y., 1972.
9. K.J. Fraser, W. Uru, W. Wiblin, AIME Light Metals 1990, pp 285.
10. K. Grjotheim, B.J. Welch, Aluminium Smelter Technology, 2nd Ed., Aluminium-Verlag, Dusseldorf, 1988.
11. K. Grjotheim, C. Krohn, M. Malinovsky, K. Matiasovsky, J. Thonstad, Aluminium Electrolysis - Fundamentals of the Hall-Heroult Process, 2nd Ed., Aluminium-Verlag, Dusseldorf, 1982.
12. X. Wang, R. Peterson, N. Richards, AIME Light Metals 1991, pp 323.
13. W.D. Zhang, J.J.J. Chen, M.P. Taylor, Proc. 18th Aust. Chem. Eng. Conf. - Chemeca, pp 1-8, 27-30th Aug (1990).
14. W.D. Zhang, J.J.J. Chen, M.P. Taylor, B.J. Welch, Proc. 19th Aust. Chem. Eng. Conf. - Chemeca, in print (1991).

ACKNOWLEDGMENTS

We wish to thank staff of the Comalco Bell Bay Smelter for their assistance in the radiotracer test-work and David Billinghurst of Comalco Research for his assistance with the mathematical proof of the effect of variation on current efficiency.